The interaction of pH, pore solution composition and solid phase composition of carbonated blast furnace slag cement paste activated with aqueous sodium monofluorophosphate

Josepha Kempl*, Oğuzhan Çopuroğlu

Delft University of Technology, Materials & Environment (CiTG), Delft, The Netherlands

* j.kempl@tudelft.nl

Abstract

Blast Furnace Slag (BFS) is a waste product of industrial steel production and a common additive in the cement industry in Northern European countries. However, cementitious materials made from slag-rich cement, particularly CEM III /B, are very susceptible to carbonation. Recent investigations have shown that the surface application of aqueous sodium monofluorophosphate (Na-MFP) as pre- and post-carbonation treatment can improve the surface durability of cementitious materials with a high BFS content. Significant improvements have been observed in the micro-mechanical characteristics of concrete surface and frost salt scaling resistance.

On the basis of previous studies we are investigating self-healing of blast furnace slag cement (BFSC) products treated with the inorganic self-healing agent Na-MFP from a mineralogical point of view. In this study we combine results of pore solution pH analyses and main element composition under the influence of Na-MFP with the presence of crystalline phases found in the solid aliquot of the samples. Pore solutions were investigated by inductively coupled optical emission spectrometry (ICP-OES). Solid-material investigation was performed by X-ray powder diffractometry, including Rietveld quantitative phase analyses.

Our results show that the element concentration and the pH of the paste pore solutions have direct influence on the formation of crystalline and amorphous phases forming in the solid sample aliquot during carbonation and self-healing by Na-MFP. In this work we focus especially on the influence of sulfur in solution and the formation of ettringite. In addition we discuss, why the formation of the crystalline phosphate apatite does not occur in cementitious products after Na-MFP treatment.

Keywords: blast furnace slag cement, sodium monofluororphosphate, X-ray diffractometry, amorphous calcium phosphates

I. Introduction

Sodium monofluorophosphate, also known as Na-MFP (chemically Na_2PO_3F) has previously been used as an inorganic corrosion inhibitor for steel reinforced concrete structures (e.g. Alonso et al. 1996). Over the past decade, Na-MFP has gained interest as an inorganic self-healing agent on cementitious products rich in blast furnace slag.

BFSC is an important product of the cement industry in Northern European countries. In the Netherlands it holds a market share of about 60% and besides many technical advantages it is an environmentally friendly product. However, its carbonation rate is a huge drawback compared to ordinary Portland cement (OPC) performances and requires a large-scale industrial and feasible solution to keep BFSC equally attractive for the building industry. Taylor (1997) explained the mechanisms of the poor carbonation resistance by shrinkage of the cement matrix, which occurs during the carbonation of a hydrated BFSC product. Due to the loss of chemically-bound water during carbonation, the matrix shrinkage induces micro-cracking. Progressing attack through environmental impact and seasonal temperature variations lead to large-scale surface damage in BFSC products and influences their life-time durability significantly.

In order to avoid this specific damage, recent experimental studies revealed the recovering effect of Na-MFP on the microstructure of carbonated BFSC pastes with respect to their frost-salt scaling durability (Çopuroğlu et al. 2006; Sisomphon et al. 2009; 2010a, 2010b). On the basis of preliminary

results, further research about the compatibility of Na-MFP for the self-healing materials concept is developed at present and adjusted to the specific slag-bearing cement type CEM III /B.

In this experimental study we are investigating the influence of cementitious pore solutions to the formation of crystalline and amorphous phases. Blast furnace slag cement pastes, particularly made of CEM III /B, were impregnated with a 45 wt% aqueous solution of Na-MFP under vacuum conditions. Pore solutions were extracted with a high-pressure apparatus previously described by Barneyback & Diamond (1981) or Byfors et al. (1986). Subsequently pore solutions and paste powders were prepared for OES-ICP and X-ray powder diffraction (XRPD).

II. Experiments

Cement paste specimens were prepared from CEM III /B (42.5N HSR LH) with a BFS content of 67 wt%; and for reference purposes from CEM I (32.5 R). Both cement types were produced by the Dutch cement manufacturer ENCI and processed according to previous experimental studies (Sisomphon et al. 2009, 2010a, 2010b). The water-cement-ratio (W/C) was chosen to be 0.45. For paste preparation common tap water was used for mixing in a commercial Hobart mixer with one minute low-speed and one minute high-speed mixing. Specimens were cast in commercial polyethylene jars. A detailed working scheme is shown in Figure 1. All pastes were cured in the fog room at 100% relative humidity (RH) for 28 days after demolding from the polyethylene jars after 24 hours. Subsequently the samples were sawn in slices of 1 cm thickness in order to ensure complete chemical reaction during the different cycles of chemical treatment.

For carbonation sample aliquots were exposed to a 3% CO_2 and a 75% RH atmosphere. For the Na-MFP treatment solutions of Na-MFP were prepared from tap water with 45 wt% Na_2FPO_3. The paste samples were vacuum impregnated with the respective solution either before or after carbonation. Chemical reaction times of 28 days were given to the specimens after Na-MFP treatment or carbonation, respectively. Between the treatments samples were stored in an oxygen free atmosphere at room temperature conditions in a 55% RH desiccator.

For every chemical treatment a reference sample was stored in the desiccator during the whole study. This results in reference sample materials of an ordinarily hydrated CEM III /B paste, a carbonated CEM III /B paste and a CEM III /B paste vacuum impregnated with the Na-MFP self-healing agent. The hydrated CEM I paste specimen is added to the present dataset for analytical comparison of the X-ray refinements. A sample list with specific steps of chemical treatment is given in Table 1.

Pore solutions of all samples were gained by the application of a high-pressure apparatus and a pressure load of up to 500 tons for each paste specimen. The TU Delft CiTG block tester (MacBen-type) with an oil-hydraulic end-load capacity of 5000 kN was used to insert a steel-cylinder assembly with an inner diameter of 34 mm and a height of 115 mm exactly fitting the size of the paste cylinders prepared in the polyethylene jars. The steel cylinder assembly was build in-house from the noble-steel type 34CrNiMo6 with a maximum tensile strength of 1400 N/mm^2 to avoid high-pressure phase transitions of the steel during exposure of the material to high pressures. The experimental set up was adapted from Barneyback & Diamond (1981).

From all paste samples a powder aliquot of five gram was taken and finely ground under ethanol in an agate mortar down to a finish of 5 μm. Samples were prepared as dry powders for X-ray powder diffraction on an aluminum sample holder.

III. Analyses

In this study the pH was analyzed with a "827 pH lab" pH meter of the Metronohm AG, Switzerland. The pH meter was calibrated with Metronohm pH buffer solutions of pH 4 and 9 at 25°C prior to the analyses.

The main element concentrations of the pore solutions were analyzed with a VARIAN Vista 720 ICP-OES. The instrument was calibrated with a 1% v/v HNO_3 blank solution and differently concentrated solutions of the commercial multi-element standard for main elements, trace elements and rare earth elements (111355 Merck IV). All samples, the standard and the procedural blanks were analyzed in 1% v/v HNO_3. The detection limit of the analyzed elements was below or equal to 200 ppb.

XRPD was performed on a Philips PW 1830/40 powder diffractometer in the micromechanical laboratory (Microlab) of Delft University of Technology (TUD). The machine is operated with an accelerating voltage of 40 kV and an X-ray beam current of 30 mA. The X-ray source is a Cu-tube working with characteristic CuKα wavelength of 0.15418 nm. The machine is equipped with a Ni-filter. Analyses were performed in air on hydrated, carbonated and on Na-MFP treated and finely ground paste powders with a stepsize of 0.02° for a 2θ angle range between 5° and 70°. Every step was analysed for 10 seconds.

A total number of 3099 data points per sample could be used for quantitative phase analyses performed by the Rietveld-refinement method with the GSAS software package. For the Rietveld-refinement an eight-term Chebeyshev polynomial model was used. Structure models for the identi-

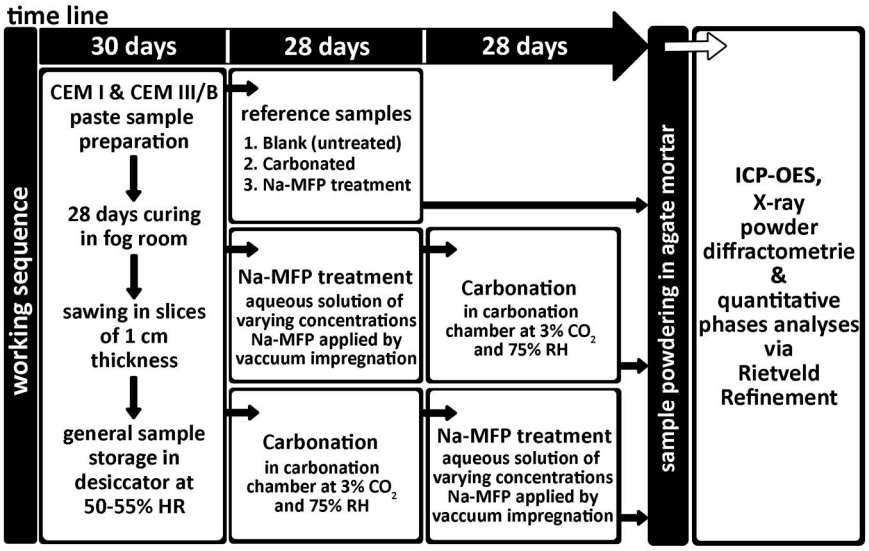

Figure 1: Schematic of working sequence and experimental treatments on cement pastes of CEM I and CEM III /B.

feid phases were taken from the Crystallography Open Database and are listed with their database number and reference in Table 2. For the identification of the C(A)SH phases, several different C(A)SH polymorphs (hillebrandite, afwillite, 14-Å-tobermorite and hydrogarnet) were used for the refinement. The polymorphs vary in their Ca:Si ratio or their water concentration, or both. C(A)SH polymorphs were primarily chosen on the basis of their peak occurrence. Due to their partly poor crystallinity and often low intensity, and due to their overlapping diffraction bands in the XRD patterns the C(A)SH phases were secondarily chosen after their Ca:Si ratio and their water concentrations as Ca and Si are to different amounts available for C(A)SH formation in each cement type. The refined phase specific parameters of the distinct crystalline and major phases were the lattice parameters, the peak profile parameters and the scale factors. Due to the high amount of amorphous phases in the BFS pastes, but also to the high band of bremstrahlung in the diffractograms between 5° and 20° 2θ (Figure 3) the occupancy factors of the ions in the solid solution series were not refined. In order to model the peak shape and the variation of the peak shift for distinct and major criystalline phases the pseudo-voigt function was chosen. The pseudo-voigt Lorentzian-Gaussian mixing parameter was refined and peak assymetry correction was also performed, again only for distinct and major crystalline phases. Finally, spherical harmonic preferential orientation corrections were applied for cylindric and platy mineral phases (portlandite, ettringite, C_3S and partially C_2S). To avoid excessive deviations, constraints were put on the lattice parameters and the profile fitting parameters with a 2% allowance for the deviation from literature values for the lattice parameters.

IV. Results and Discussion

Analyses of pH and main elements

The pH of all cement paste pore solutions is listed in Table 3. As expected, the hydrated cement pastes have a very basic character with a pH of 13.1 for CEM I and 13.0 for CEM III /B. The carbonated CEM III /B paste pore solution has a pH of 8.8. These results are in good agreement with the commonly analyzed pH values of ∼13 for hydrated cement pastes and 8-9 for carbonated cement pastes (e.g. Taylor, 1997). If an aqueous solution of 45 wt% Na-MFP is added to the CEM III /B paste via vacuum impregnation, the pH of the pore solution is increasing to a pH of 13.1 (Table 3). In the framework of corrosion inhibition, especially Na has been

Table 1: Sample list showing sample ID, chemical treatment and sample age of each specimen.

sample ID	treatment	sample age [d]
CEM I-01	hydrated CEM I	30
CEM III-01	hydrated CEM III /B	30
CEM III-02	hydrated & carbonated CEM III/B	58
CEM III-06	hydrated & 45% Na-MFP impregnated CEM III /B	58
CEM III-08	hydrated, carbonated & 45% Na-MFP impregnated CEM III /B	86

Table 2: Phase names, mineralogical formulas, abbreviations, cement chemistry notation (CCN) and the crystallographical open database (COD) reference number as well as the literature references of the phases used during Rietveld-refinements.

phase	formula	abbrev.	CCN	COD no.	reference
cement paste phases					
portlandite	$Ca(OH)_2$	po	CH	1008780	Busing & Levy (1957)
alite	Ca_3SiO_5		C_3S	9016125	De la Torre et al. (2008)
belite	Ca_2SiO_4		C_2S	9014595	Udagawa et al. (1980)
ettringite	$Ca_6Al(SO_3)_4(OH)_{12}\cdot 26H_2O$	et	$C_6A\bar{S}_3H_{32}$	9015084	G.-Neunhoffer & Neubauer (2006)
melilite	$(Ca,Na)_2(Al,Mg,Fe^{2+})[(Al,Si)SiO_7]$	me		9000055	Smith (1953)
aragonite		arg		9000226	De Villiers (1971)
calcite	$CaCO_3$	cc	$C\bar{C}$	9000095	Graaf (1961)
vaterite		vat		9007475	Wang & Becker (2009)
C-(A)-S-H phases					
afwillite	$Ca_3[SiO_3OH]_2\cdot 2H_2O$		C_3SH_5	9007428	Megaw (1952)
hillebrandite	$Ca_6[Si_3O_9](OH)_6$		C_6S_3H	9001698	Dai & Post (1995)
hydrogarnet	$Ca_3Al_2[SiO_4)_{3-x}(OH)_{4x}]$		C_3AH_6	1007235	Cohen-Addat et al. (1964)
tobermorite (14Å)	$Ca_5[Si_6(O,OH)_{18}]\cdot 5H_2O$		$C_5S_6H_{28}$	9013974	Bonaaccorsi & Merlino (2005)

shown to be responsible for the increase of the pH (e.g. Jin et al. 1991). The CEM III /B paste that was first carbonated and subsequently impregnated with the Na-MFP solution has a pH of 11.7. This shows that the treatment of a slag-rich carbonated cement paste with a 45 wt% solution of Na-MFP has the potential to recover the pH of a hydrated CEM III /B with up to 90% in a chemical reaction time of 28 days.

The results of the main element analyses are also listed in Table 3. In order to illustrate the percentage of main element concentrations in the slag-rich cement pastes, the relative main element concentrations are shown in pie diagrams in Figure 2. In the pore solution of a hydrated CEM I (CEM I-01) paste the alkali elements Na^+ and K^+ make up the highest concentration with 44.6wt.% and 52.2wt.%, respectively and stabilize the very basic pH, while Mg^{2+}, Ca^{2+}, S^{4+} and the trace elements (Li, Ba, Sr, Fe, Al and Si) comprise a total of 3.2%. The high amount of alkali elements has previously also been observed by Song & Jennings (1999) and Brouwers & van Eijk (2003). A similar result was analysed in the hydrated CEM III /B (CEM III-01) paste in which Na^+ makes up about 48.5% and K^+ makes up 46.3% of the main elements in the pore solution. The remaining 5.2% consist of Mg^{2+}, Ca^{2+}, S^{4+} and the trace elements. In CEM I pastes as well as in CEM III /B pastes the high pH is controlled by the high concentrations of alkali elements (Song & Jennings, 1999; Brouwers & van Eijk, 2003). The increase of S^{4+} in the pore solution of a slag-rich cement paste compared to the pore solution of a hydrated CEM I paste can be explained by the presence of BFS containing an additional amount of S^{4+}.

The main element concentrations in a slag-rich cement paste change drastically after carbonation (CEM III-02); especially the concentration of S^{4+} is increasing remarkably with up to 53.6% in the pore solution. Also Ca^{2+} (28.2%) and Mg^{2+} (13.1%) are increasing in the pore solution of a carbonated CEM III /B paste, while Na^+, K^+ and the trace elements can be summed up to 5.1%. If a hydrated CEM III /B paste is impregnated with a 45 wt% solution of Na-MFP (CEM III-06), an increase of Na^+ (65.1%) must be obvious. Relative to Na^+, K^+ makes up about 23.7%, while Mg^{2+}, Ca^{2+}, S^{4+} and the trace elements result in a total percentage of 11.3% and seem to be getting activated by Na-MFP. Again, expecially S^{4+} is remarkably increasing in the pore solution. Finally, the Na^+ concentration in a carbonated CEM III /B paste impregnated with Na-MFP solution (CEM III-08) increases up to 57.1%. While K^+, Mg^{2+}, Ca^{2+} and the trace elements make up 2.4%, S^{4+} is again present as a major element with up to 39.8%.

The relatively high concentrations of the main elements in the two CEM III /B cement pastes (Table 3) treated with Na-MFP solutions are mainly caused by the Al^{3+} and $Fe^{3+/2+}$, likely being activated with the addition of Na-MFP.

X-ray powder diffraction and quantitative phase analyses by Rietveld-refinement

Prior to the quantitative phase analyses occurring crystalline phases were identified. The x-ray diffractograms of all samples are shown in Figure 3. The diffraction pattern of hydrated CEM I paste was

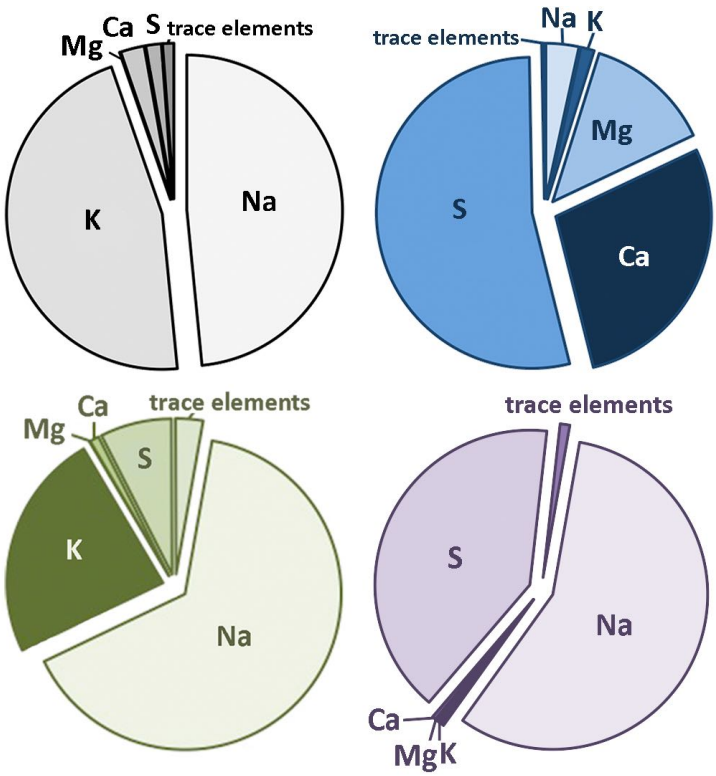

Figure 2: Main element concentrations of slag-rich cement paste pore solutions in percent; upper left: hydrated CEM III /B; upper right: hydrated and carbonated CEM III /B; lower left: Na-MFP impregnated CEM III /B and lower right: carbonated and Na-MFP impregnated CEM III /B.

primarily added for reference purposes. Distinct peaks of crystalline phases such as portlandite, ettringite and alite could clearly be identified and were used for further preliminary peak identification in the slag-rich cement paste diffractograms. Less distinct peaks of belite could also be found, but were partly overlapped by alite (Taylor, 1997), which can form solid solutions with Mg^{2+}, $Al^{3}+$, P^{4+}, Fe^{2+} and Si^{4+} (Nishi et al. 1984). Due to their poor crystallinity, but also to their complex solid solution formation with alkali elements and the occurrence of numerous polymorphs and varying water concentrations, the C(A)SH phases could not clearly be identified. The primarily amorphous character of these phases also causes a relatively large background and a diffuse diffraction band between 25° and 40° 2θ. However the refinement was performed with afwillite and 14-Å tobermorite, of which afwillite was found to be the major CSH-phase, while tobermorite was quantified with an amount of less than 2 wt%, which is below the actual detection limit of the method. The results of the quantitative analyses are listed in Table 4.

X-ray diffraction patterns of slag-rich cement pastes generally show a diffuse, asymmetric band from the amorphous blast furnace slag ranging from 20° to 48° 2θ and peaking at about 31° 2θ (Regourd, 1986). In addition the diffuse band of the poorly cristalline to amorphous CSH phases is underlying the amorphous BFS band in the diffraction pattern in Figure 3. This even increases the background of the diffraction patterns for the slag-rich cement pastes.

However in a hydrated CEM III /B (CEM III-01)

Table 3: pH values and main element concentrations of the pore solutions gained from high-pressure pore solution expression. The trace elements are a total of Li, Ba, Sr, Fe, Al, and Si.

sample ID	Elements dissolved in pore solution [mg/l]						
	pH	**Na**	**K**	**Mg**	**Ca**	**S**	**trace elements**
CEM I-01	13.1	2277.1	2662.9	0.5	110.9	15.6	35.9
CEM III-01	13.0	1630.9	1557.1	0.5	83	54.4	39.8
CEM III-02	8.8	229.3	93.8	877.9	1881.3	3582.6	18.7
CEM III-06	13.1	5069.3	1841.7	4.36	74.43	576.81	220.9
CEM III-08	11.7	24124.3	397.5	12.23	177.3	17100.7	430.4

paste distinct peaks of ettringite and portlandite could clearly be identified. Wider peaks of alite (31°-33° 2θ), and a diffuse mixture of portlandite and ettringite bands (27°-29° 2θ) could be observed and were used for the quantitative phase analyses. The amount of portlandite quantified in CEM III /B is approximately three times lower than the amount of portlandite in the comparable CEM I paste (Table 4). This is in good agreement with the starting composition of the cement types: blast furnace slag cement contains about 67 wt% BFS and therefore roughly one-third less clinker. Consequently, only about one-third of CaO can undergo hydration during paste manufacturing and curing in CEM III /B. The analyses of the slag-rich cement paste resulted in a relatively high concentration of alite (71.3 wt%). Though a higher amount of alite could be expected in slag-rich cement pastes, due to the higher concentration of Si in the BFS, this value is unusally high. It might be caused during the refinement as a consequence of overlapping peaks with belite or the large peak width on top of the amorphous CSH fraction of the sample. The latter has likely happened since it is visible in the relatively low amount of quantified crystalline CSH phases (Table 4). CEM III /B has a much larger chemical variability due to the addition of BFS, which generally has a melilitic composition. As a result the formation of portlandite solid solition e.g. with the isostructural brucite (mineralogically $Mg(OH)_2$) and additional dipositive ions would be expected (Taylor, 1997 and references therein). In addition, the poorly crystalline CSH phases can substitute a couple of ions. In a gel or amorphous phase these ions can even multiple-positively be charged. In general this includes minor amounts of Al^{3+}, $Fe^{3+/2+}$, Al^{3+}, Si^{4+}, K^{+}, Na^{+}, but it can also comprise ions such as P^{4+} (Taylor, 1997). The non-stoichiometric amorphous amount of phases existing in the samples surely tamper with the phase quantification.

With the addition of aqueous Na-MFP to a hydrated slag-rich cement paste (CEM III-06) the ettringite peaks show a slightly higher intensity compared to the hydrated CEM III /B paste. The quantitative analyses resulted in 15 ($\pm$2) wt% ettrinigite compared to the hydrated slag-rich cement paste. The amount of portlandite in CEM III-06 is given with 9 wt%, which scatters within the common standard deviation of $\pm$2 wt% for each clearly crystalline quantified phase. Compared to the hydrated slag cement paste the amount of portlandite is not significantly varying. C(A)SH phases chosen for

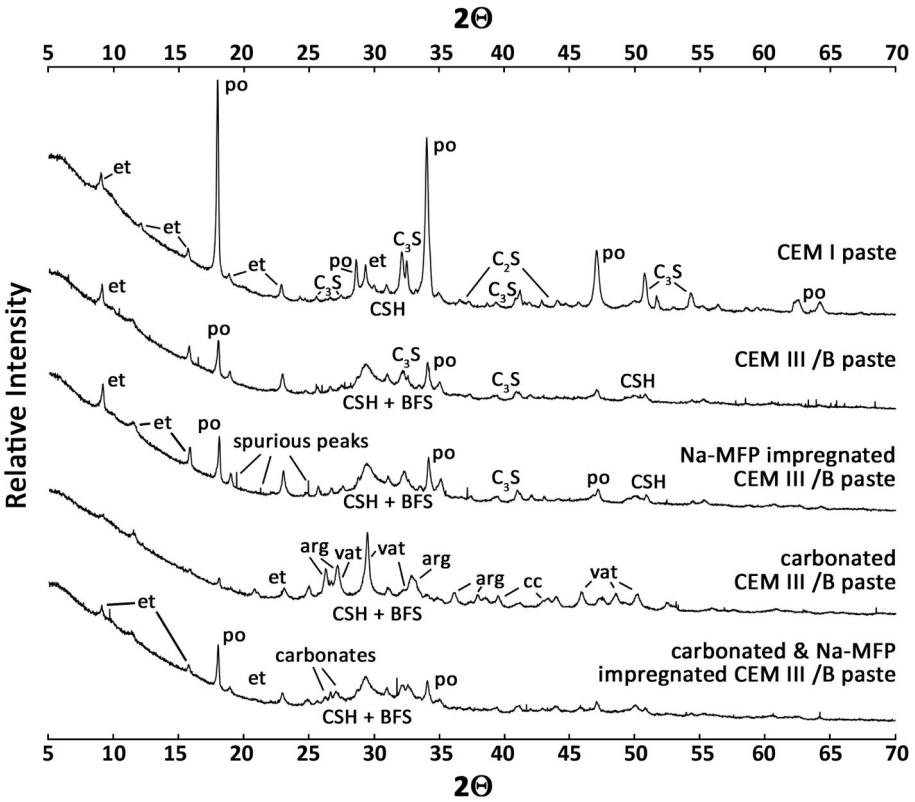

Figure 3: X-ray diffrcation patterns of the cement pastes investigated in this study; from top to bottom CEM I-01, CEM III-01, CEM III-02, CEM III-06 and CEM III-08. Some crystalline phases, such as portlandite, ettrinigite, alite, vaterite, calcite and aragonite show distinct peak positions, whereas poorly cristalline phases, amorphous phases or phases with a lower quantity cause a rather high background or broad peaks, respectively.(see Table 2 for mineral abbreviations).

Table 4: Results of the quantitative phase analyses by Rietveld-refinement. The standard deviation for the amount of distinct crystalline phases is ±2 wt% in a refinement with about 100% of a crystalline sample.

sample ID → **sample treatment →**	**CEMI-01 hyd**	**CEM III-01 hyd**	**CEM III-02 hyd, cc**	**CEM III-06 hyd, Na-MFP imp**	**CEM III-08 hyd, cc, Na-MFP imp**
Statistical parameters of the Rietveld refinement					
R_P	0.023	0.032	0.03	0.025	0.024
R_{WP}	0.039	0.043	0.042	0.043	0.041
DWD	0.414	0.507	0.657	0.7	0.593
χ^2	5.696	7.948	4.389	5.478	4.798
Results of the quantitative phase analyses of the crystalline phases in wt%					
Portlandite	32	10	3	9	7
Alite	23	71	22	18	18
Belite	3		6	7	
Ettringite	13	13	7	15	15
Melilite		2			
Aragonite			18		
Calcite			19		13
Vaterite			25		10
crystalline C-(A)-S-H	29	2		51	36

the refinement were hillebrandite (17 wt%), 14-Å tobermorite (26 wt%) and hydrogarnet (8 wt%). These phases were chosen due to there smaller Ca:Si ratio in comparison to afwillite and due to their better compatibility in the course of the refinement. Again the C(A)SH phases can substitute numerous positively charged ions in the form of a non-stoichiometric gel.

After carbonation of a hydrated CEM III /B paste (CEM III-02), the distinct peaks of portlandite disappear almost completely (Figure 3). The amount of portlandite quantified in this sample is 3 (±2) wt% (Table 4). Also the intensity of the ettringite peaks is clearly decreased after carbonation. The quantified crystalline amount in this sample is 7 (±2) wt%. Instead of distinct ettringite and portlandite peaks, large amounts of vaterite, aragonite and calcite were identified (Table 4) amongst the crystalline fraction of the sample. This is in good agreement with the observations by Brocken & Nijland (2004), who assume the formation of vaterite after the interaction of carbon dioxide with ettringite during carbonation. Crystalline CSH phases have not been detected and the diffuse band of CSH phases seems to be decreased in the diffraction pattern of CEM III-02. Greenberg & Chang (1965) found CSH phases to be instable at pH values below 9.5. This finding would be in good agreement with the absence of CSH phases in the diffraction pattern and the analysed pH of 8.8 (Table 3). Alite and belite do not seem to be significantly influenced by the rather short time period of hydration and carbonation given to the sample in this study.

CEM III-08 was first carbonated and subsequently impregnated with aqueous Na-MFP. The diffraction pattern shows a recovery of portlandite from 3 (±2) wt% in the carboanted cement paste to 7 (±2) wt% in the sample that was first carbonated and subsequently impregnated with Na-MFP. It also shows a decent re-occurence of the ettringite peaks, quantified with about 15 (±2) wt% of the crystalline fraction of the samples and a re-occurrence of the diffuse diffraction band of the CSH phases (36 (±2) wt%) after the recovery of the pH up to 11.7 (Table 3). The dominant CSH phase chosen for the refinement was 14-Å tobermorite. The clinker crystal alite seems to be stable during the whole carbonation and Na-MFP impregnation process within the investigated sample age, while belite could not be identified in this sample. Instead a decent total percentage of carbonates of 23 (±2) wt% is still present.

Rietveld-refinement and its challenges to cement product analyses

The Rietveld-refinement method generally allows quantitative phase anlayses of crystalline materials. Thanks to the development of high-performance X-ray powder diffractometers and detectors as well as stable-functioning software, improved sample preparation techniques and analyses, the Rietveld refinement has become a common tool in the cement, cement clinker and cement product characterization. However, a Rietveld refinement has not become a trivial analysis. Specific issues of quantifying hydrated cement phases are the occurrence of numerous poorly crystalline or even amorphous phases such as CSH phases. Some of them are

only present in minor amounts of less than 2 wt%; which is just the detection limit for a crystalline phase in a good quality refinement. Additionally the occurrence of overlapping diffraction peaks, as well as the common paragenesis of solid solution series and polymorphs of occurring hydrated cement phases as well as the occurrence of other amorphous supplementary cementitious materials such as BFS, influence the statistical quality parameters of a refinement on cementitious composites.

In the refinement presented in this study the DWD and χ^2 of each analyses did not reach the necessary values to speak about a 90% certainty for phase quantification (Table 4). This is mainly due to the amounts of amorphous BFS and the formation of poorly crystalline C(A)SH phases, increasing the background of the analyses. In addition the Philips pw 1830/40 is a relatively old machine showing the large band of bremsstrahlung between 5° and 20° 2θ in the diffractograms (Figure 3). After the analyses of a 98% crystalline quartz standard, the same band has been observed and could be excluded to be purely caused by the presence of amorphous phases.

Due to the available equipment and filters we consciously disclaimed the refinement of the occupancy factors of the ions in the occurring solution series and the subtraction of the amorphous phases as suggested by Snellings et al. (2014a; 2014b). In addition, the diffraction patterns show numerous spurious peaks originating from the tungsten of the old X-ray tube that also influences the statistical parameters of the quantitative phases analyses. In this context it should be mentioned that our results "only" show the crystalline phases included in the analyses and that the sums are normalized up to the phase contents of 100% as usually performed by the refinements. That means that only relative proportions of the crystalline phases are obtained, while the amorphous fraction of the samples should better be identified by e.g. electron-microscopy and image analysis.

The concentration of magnesium in pore solution and the presence of apatite

The acidic character and composition of a cementitious paste pore solution has a strong influence on the stabilization or destabilization of crystalline and amorphous phases. In this context hydration and carbonation processes of numerous cement types have intensively been studied (e.g. Hong & Glasser, 2002; Bullard et al. 2011).

Yet, several studies have controversially discussed the formation of apatite (Çopuroğlu et al. 2006; Zemskov S.V. et al. 2012; Söylev & Richardson, 2008; Douche-Portanguen et al. 2005; Farcas et al. 2002; Bastidas et al. 2010; Tadic et al. 2002), based on results of experimental work that have shown that the crystalline calcium phosphate with the mineral formula $Ca_5(PO_4)_3(OH/F/Cl)$ can form from portlandite and Na-MFP in aqueous solutions of different pH values (Farcas et al. 2006, Bastidas et al. 2010). Yet, the formation of apatite after Na-MFP treatment of BFSC products has never been observed (Sisomphon et al. 2011; Douche-Portanguen et al. 2005) and could also not be justified by thermodynamic calculations (Bastidas et al. 2010). Although the occurrence of apatite-like structures was earlier detected in calcium aluminate cements by Pöllmann (2012), neither hydroxyl- nor fluoroapatite could ever be identified in cementitious products treated with Na-MFP (Alonso et al. 1996; Çopuroğlu et al. 2006; Söylev & Richardson, 2008; Douche-Portanguen et al. 2005). Instead, the interaction of hardened cement paste with Na-MFP in solution resulted in the formation of portlandite, carbonates and a paragenisis with clinker minerals (Douche-Portanguen et al. 2005) and non-stoichiometric amorphous calcium phosphates (Çopuroğlu et al. 2006) or traces of $FePO_4{\cdot}H_2O$ (Alonso et al. 1996; Söylev & Richardson, 2008) in the environment of steel reinforcements.

Boskey and Posner (1974) experimentally investigated the conversion of Amorphous Calcium Phosphate (ACP) to hydroxyl-apatite in the presence of magnesium and found very low concentrations of magnesium already influencing the amorphization of apatite. The concentrations of Mg^{2+} presented in Table 3 are sufficient to prevent the formation of crystalline apatite in cementitious products. The results of the X-ray powder diffraction analyses also confirm that no crystalline phosphate mineral is formed during Na-MFP treatment of portlandite-bearing cementitious products – at least not within the age and time range of sample investigation.

Sulfur in pore solution, carbonation and the stability of ettringite

The results of the main element analyses (Table 3) show that S^{4+} in a carbonated slag-rich cement paste pore solution is increasing to an amount of 3.5 g/l compared to the non-carbonated slag-cement paste. Correlating this result with the result of the crystalline phase analyses (Table 4) we observe the amount of the crystalline sulfur-bearing mineral ettringite, as formed during cement hydration, to be decreasing by progressing carbonation. That way S^{4+} can be released to the pore solution. Brocken & Nijland (2004) assume that during carbonation vaterite and possibly other carbonates are forming from ettringite and carbon dioxide, but do not discuss to where sulfur could partition. Though S^{4+} can be bound to amorphous hydration products

(C(A)SH phases) in cement pastes, the amount of S^{4+} in the pore solution of the carbonated slag-cement paste is significantly high. This again can be explained by the pH of a carbonated paste (in this case 8.8) and the fact that only at pH values higher than 9.5 the C(A)SH phases are stable. The high sulfur concentration in the pore solution of a carbonated CEM III /B paste is a result of ettringite dissolution.

Brocken & Nijland (2004) show an SEM photomicrograph, illustrating the formation of ettringite needles that preferably occur at the interface between pore paste surface and paste matrix. If ettringite breaks down during carbonation, sulfur is increasing especially in the pore solutions.

V. Conclusion

Through the application of aqueous Na-MFP as a self-healing agent on CEM III /B this study shows that Na-MFP has the potential to recover the pH of a carbonated cement paste up to 90% with an Na-MFP concentration of 45 wt% in the healing agent.

Parallel to our solid-phase analytical results we show that during carbonation of a slag-rich cement paste phase transitions from portlandite, ettringite and C(A)SH occur to form carbonates such as vaterite, aragonite and calcites, while the clinker phases do not show a large reactivity in the time period of sample investigation.

The influence of Na-MFP on a carbonated cement paste is stabilizing secondary portlandite, ettringite and C(A)SH, possibly due to recovery of the basic character of the pore solution. Diffraction peaks of the crystalline phosphate mineral apatite were not observed within the time period of sample investigation and are also not expected to occur at any later sample age. The latter assumption is underpinned by the existence of several studies on thermodynamic calculations, the high pH destabilizing apatite and by the existence of Mg^{2+} in the pore solution.

Future work by polarized light and electron microscopy will give more insight in the composition of the Amorphous Calcium Phosphates (ACP's) that are forming in paragenesis with C(A)SH phases in slag-rich carbonated cement paste treated with the inorganic self-healing agent Na-MFP.

Acknowledgement

We would like to express our gratitude to the Dutch Enterprise Agency (Agentschap.NL) who kindly supported this work financially through the IOP Self Healing Materials (SHM) Program.

References

Alonso C., Andrade C., Argiz C., Malric B. (1996) "Na2PO3F as inhibitor of corroding reinforcement in carbonated concrete" Cement and Concrete Research; 26: 405-415.

Barneyback R.S., Diamond S. (1981) "Expression and Analyses of Pore solutions from hardened Cement Pastes and Mortars" Cement and Concrete Research; 11: 279-285.

Bastidas D.M., La Iglesia V.M., Criado M., Fajardo S., La Iglesia A., Bastidas J.M. (2010) "A prediction study of hydroxyapatite entrapment ability in concrete" Constr Build Mater; 24: 2646-2649.

Bonaccorsi E., Merlin S. (2005) The crystal tobermorite 14 A (plombierite) phase locality: Ballycraigy, Northern Ireland" Journal of the American Ceramic Society; 88, 505-512.

Boskey A.L., Posner A.S. (1974) "Magnesium stabilization of amorphous calcium phosphate: A kinetic study" Material Research Bulletin; 9: 907-916.

Brocken H., Nijland T.G. (2004) "White efflorescence on brick masonry and concrete masonry blocks, with special emphasis on sulfate efflorescence on concrete blocks" Construction and Building Materials; 18, 315-323.

Brouwers H.J.H., van Eijk R.J. (2003) "Alkali Concentrations of Pore Solutions in hydrating OPC" Cement and Concrete Research; 33: 191-196.

Bullard J.W., Jennings H.M., Livingston R.A., Nonat A., Scherer G.W., Schweitzer JS, Scrivener K.L., Thomas J.J. (2011) "Mechanisms of Cement Hydration" Cement and Concrete Composites; 41: 1208-1223.

Busing W.R., Levy H. (1957) "A Neutron diffraction study of calcium hydroxide" Journal of Chemical Physics; 26, 563-568.

Byfors K, Hansson CM, Tritthart J. (1986) "Pore Solution Expression as a Method to determine the Influence of Mineral Additives on Chloride Binding" Cement Concrete Res; 16: 760-770.

Cohen-Addad C., Ducros P., Durif A., Bertaut E.F., Delapalme A. (1964) "Determination de la position des atomes d'hydrogene dans I'hydroginat Al2O3, (CaO)3 (H2O)6 par resonance magnetique nucleaire et diffractionique" Journal de Physique; 25, 478-483.

Çopuroğlu O., Fraaij A.L.A., Bijen JMJM. (2006) "Effect of Sodium monofluorophosphate treatment on microstructure and frost salt scaling durability of slag cement paste" Cement and Concrete Research; 36: 1475-1482.

Dai Y.S., Post J.E. (1995): "Crystal structure of hillebrandite: A natural analogue of calcium silicate hydrate (CSH) phases in Portland cement" American Mineralogist; 80: 841-844.

De la Torre A.G., De Vera R.N., Cuberos A.J.M., Aranda M.A.g. (2008) "Crystal Structure of low magnesium-content alite: Application to Rietveld quantitative phase analysis" Cement and Concrete Research; 38, 1261-1269.

De Villiers (1971) "Crystal structures of aragonite, strontianite, and witherite" American Mineralogist; 56, 758-767.

Douche-Portanguen A., Prince W., Malric B., Arliguie G. (2005) "Study of interactions between sodium monofluorophosphate and hardened cement paste and their consequences on concrete transfer properties" Cement and Concrete Research; 35: 1714-1723.

Farcas F., Chaussadent T., Fiaud C., Mabille I. (2002) "Determination of the sodium monofluorophosphate in a hardened cement paste by ion chromatography" Anal. Chim. Acta 472: 37-43.

Goetz-Neunhoeffer F., Neubauer J. (2006) "Refined ettringite (Ca6Al2(SO4)3(OH)12*26H2O) structure for quantitative X-ray diffraction analysis" Powder Diffraction; 21, 4-11.

Graf D.L. (1961) "Crystallographic tables for the rhombohedral carbonates" American Mineralogist; 46, 1283-1316.

Hong S-Y., Glasser F.P. (2002) "Alkali sorption by CSH and CASH gels Part II. Role of Alumina" Cement and Concrete Composites; 32: 1101-1111.

Jin S.X., Sagoe-Crentsil K.K., Glassert F.P. (1991) "Characteristics of corrosion inhibition admixtures in OPC paste with chloride additions. Part I: Chemistry and electrochemistry." Magazine of Concrete Research; 43: 205-213.

Megaw H.D. (1952): " The structure of afwillite, Ca3[SiO3OH]2●2H2O Locality: Scawt Hill, Northern Ireland" Acta Crystallographica; 5: 477-491.

Nishi F., Takeuchi Y., Maki I. (1984) "The tricalcium silicate Ca3OSiO4: The monoclinic superstructure" Zeitschrift für Kristallographie; 172, 297.

Pöllmann H. (2012) "Calcium Aluminate Cements – Raw Materials, Differences, Hydration and Properties" Reviews in Mineralogy and Geochemistry; 74: 1-82.

Regourd M. (1986) "Caracterisiques et activation des produits d'addition" Proc. 8th ICCC; 1, 199. Rio de Janeiro, Brasil

Schellings R., Salze A., Scrievener K.L. (2014a) "Use of X-ray diffraction to quantify amorphous supplementary cementicious materials in anhydrous and hydrated blended cements" Cement and Concrete Research; 64: 89-98

Schellings R., Salze A., Scrievener K.L. (2014b) "The existence of amorphous phase in Portland cements: Physical factors affecting the Rietveld quantitative phase analyses" Cement and Concrete Research; 59: 139-146.

Sisomphon K, Çopuroğlu O, Fraaij A. (2009): "Transport Properties and Frost Salt Scaling Resistance of Carbonated Blast-Furnace Slag Mortars after Sodium Monofluorophosphate Treatment" 2nd International RILEM Workshop on Concrete Durability and Service Life Planning; Haifa, Israel. 9: 138-145.

Sisomphon K., Çopuroğlu O., Fraaij A. (2010a): "Properties of carbonated blast furnace slag mortars after Na2FPO3 treatment" Science Asia; 36: 223-230.

Sisomphon K, Çopuroğlu O, Fraaij A. (2010b) "Development of Blast Furnace Slag Mixtures against Frost Salt Attack" Cement and Concrete Research; 32: 630-638.

Sisomphon K., Çopuroğlu O., Fraaij A. (2011) "Application of encapsulated lightweight aggregate impregnated with sodium monofluorophosphate as a self-healing agent in blast-furnace slag mortar" Heron; 56: 13-32.

Smith V. (1953) "Reexamination of the crystal structure of melilite" American Mineralogist; 38, 643-661.

Song S., Jennings H.M. (1999) "Pore solution of alkali-activated ground granulated blast-furnace slag" Cement and Concrete Research; 29:159-170.

Söylev T.A., Richardson M.G. (2008) "Corrosion inhibitors for steel in concrete: State-of-the-art report" Const Build Mater; 22:609-622.

Tadic D., Peters F., Epple M. (2002) "Continous synthesis of amorphous carbonated apatites" Biomaterials; 23: 2553-2559.

Taylor H.F.W. (1997) Cement Chemistry, 2nd ed., Thomas Telford, London.

Udagawa S., Urabe K., Natsume M., Yano T. (1980) "Refinement of the crystal structure of gamma-Ca2SiO4" Cement and Concrete Research; 10, 139-144.

Wang J., Becker U. (2009) "Structure and carbonate orientation of vaterite (CaCO3)" American Mineralogist; 94, 380-386.

Zemskov S.V., Ahmad B., Çopuroğlu O., Vermolen F.J. (2012) "Modeling of a self-healing process in blast furnace slag cement exposed to accelerated carbonation." IC-MSQUARE: International Conference on Mathematical Modelling in Physical Sciences; Journal of Physics: Conference Science; 410: 1-4.